Non-Darcy free convective flow along a vertical cylinder embedded in a porous medium with surface mass flux

M. A. Hossain
Department of Mathematics, University of Dhaka, Dhaka, Bangladesh

A. Nakayama
Department of Energy and Mechanical Engineering, Shizuoku University, Hamamatsu, Japan

The nonsimilar non-Darcian free-convection flow about a vertical cylinder with impermeable surface embedded in a saturated porous medium, where surface temperature of the cylinder varies as x^m, a power function of distance from the leading edge, has been studied by employing the implicit finite-difference method together with the Newton's quasi-linearization technique. In the present investigation, effects of the surface mass flux together with the inertial effects on the rate of heat transfer at the surface, on the velocity distribution, and on the temperature distribution are shown graphically.

Keywords: porous media; forced convection; non-Darcy flow; vertical cylinder; mass flux

Introduction

Convective motion in a porous medium has attracted considerable attention from several authors because of its applications in geophysics, oil recovery technique, thermal insulation, engineering, and heat storage systems (see Cheng 1978, 1984), and references cited therein). In almost all these works, the boundary-layer formulation of Darcy's law and the energy equation were used. In the non-Darcian natural convection flow, numerous investigations have been conducted (Plumb and Huenefeld 1981; Bejan and Poulikakos 1984; Hsu and Cheng 1985; Hong and Yamada 1987; Hong et al. 1985; Cheng 1981). The inertia effect has been shown to decrease the heat transfer when the Rayleigh number is increased (Plumb and Huenefeld 1981; Bejan and Poulikakos 1984). The buoyancy effect due to a no-slip boundary condition also results in a small Nusselt number, but is less pronounced as the Rayleigh number is increased (Hsu and Cheng 1985; Hong and Yamada 1987; Hong et al. 1985; Cheng 1981).

In recent years, interest has developed in the study of natural convection flow in porous media from the surfaces of various configurations. Minkowycz and Cheng (1981) were the first to study the natural convection flow about a vertical heated cylinder embedded in a saturated porous medium, considering that the surface temperature satisfies the power-law variation of the distance measured from the leading edge. With the framework of a boundary-layer approximation, exact solutions of this problem were obtained for the case in which the surface temperature varies linearly with the distance; but for the case with nonlinear variations of the surface temperature, approximate solutions based on local similarity as well as on the local nonsimilarity methods of Sparrow and Yu (1971) and Minkowycz and Sparrow (1974) were obtained. Later, Merkin (1986) investigated the problem posed by Minkowycz and Cheng (1981) using the implicit finite-difference method and the series expansion method near the leading edge as well as in the downstream, considering the fact that surface temperature varies linearly with the distance measured from the leading edge. These studies of Minkowycz and Cheng (1981) and Merkin (1986) are confined to the Darcy flow. Recently, non-Darcian natural convection from an isothermal slender vertical frustrum of a cone embedded in a saturated medium has been studied by Vasantha et al. (1986). On the other hand, Ingham (1986) has investigated a similar type of boundary-layer flow on axisymmetric and two-dimensional (2-D) bodies of arbitrary shape.

As a continuing effort towards a complete understanding of transport phenomena in porous medium, the influence of surface mass flux on the free-convection boundary-layer flow of Darcian fluid in a saturated porous medium along vertical as well as horizontal surfaces has been studied, respectively, by Minkowycz and Cheng (1981) and Minkowycz et al. (1985). Very recently, Lai and Kulacki (1990) have investigated the similarity and Kumeri et al. (1990) the nonsimilarity solutions for non-Darcian mixed convection flow about a horizontal surface with the effect of the influence of surface mass flux in a saturated porous medium. However, such extensive efforts do not exist for non-Darcian free-convection flows along a vertical cylinder subject to a variable wall temperature, in which the combined effects of the surface mass flux, variable wall temperature, and porous inertia on the heat transfer rate must be considered together with the transverse radial curvature effects.

In the present paper, we therefore propose to investigate the effect of the surface mass flux on the non-Darcy free-convection flow along a heated vertical cylinder embedded in a saturated porous medium, where the surface temperature of the cylinder varies as x^m, a power function of the distance from the leading edge. Due to complexities associated with the foregoing various

Address reprint requests to Professor Hossain at the Department of Mathematics, University of Dhaka, Dhaka 1000, Bangladesh.

Received 17 June 1992; accepted 18 November 1992

effects on the flow governed by nonsimilarity boundary-layer equations of momentum and energy, the implicit finite-difference technique together with the Keller box method appears to be most efficient for the study of the effects of flow parameters in the wide ranges. The numerical values thus obtained from the finite-difference calculations are tabulated for the wide ranges of the parameters.

Governing equations

The governing equations for the non-Darcy steady free-convection flow of viscous incompressible fluid about a vertical porous cylinder of radius r_0 embedded in a saturated porous medium with a prescribed axially symmetric wall temperature —namely, the equation of continuity, the Forchheimer equation with Boussinesq approximation, and the energy equation—can be written by using the usual boundary-layer approximation (following Plumb and Huenefeld, 1981; Minkowycz and Cheng, 1981) as

$$\frac{\partial}{\partial x}(ru) + \frac{\partial}{\partial r}(rv) = 0 \tag{1}$$

$$u + \frac{\delta K^*}{\mu} u^2 = \frac{K\delta g\beta}{\mu}(T - T_\infty) \tag{2}$$

$$u\frac{\partial T}{\partial x} + v\frac{\partial T}{\partial r} = \alpha\frac{1}{r}\frac{\partial}{\partial r}\left(r\frac{\partial T}{\partial r}\right) \tag{3}$$

where u and v are the velocity components along the x and r directions, respectively, μ, δ, and β are the viscosity, the density and the thermal expansion coefficient of the fluid, respectively; α is the thermal diffusivity; g is the acceleration due to gravity; T_∞ is the temperature of the ambient fluid; and T is the temperature in the boundary layer. In Equation 2,

$$K = \frac{D_p^2 s}{150(1-s)^2} \quad \text{and} \quad K^* = \frac{1.75 D_p}{150(1-s)} \tag{4}$$

where K and K^* are the permeability and the inertial coefficients, respectively, in terms of characteristic pore or particle diameter D_p and the porosity s. Equation 2 approaches Darcy's law for very small K^*. According to Plumb and Huenefeld (1981), the inertial effects are found to be significant when

$$\frac{g\beta KK^*(T_w - T_\infty}{v^2} > 0.1 \tag{5}$$

The appropriate boundary conditions for the present problem are

$$\left.\begin{aligned} v = V(x) = ax^\lambda,\ T = T_w = T_\infty + Ax^m \text{ at } r = r_0 \\ u = 0,\ T = T_\infty \text{ as } r \to \infty \end{aligned}\right\} \tag{6}$$

where $V(x)$ is the surface mass flux and a is positive for blowing and negative for withdrawal of fluid. In Equation 4, we have assumed that the prescribed temperature is a power function of the distance from the leading edge.

Following Minkowycz and Cheng (1981), we now introduce the following group of transformations for the dependent and independent variables:

$$\left.\begin{aligned} \eta &= \frac{\mathrm{Ra}_x^{1/2}}{2x}\left\{r_0\left(\frac{r^2}{r_0} - 1\right)\right\}, & \xi &= \frac{2x}{r_0}\mathrm{Ra}_x^{-1/2} \\ \psi &= \alpha r_0\,\mathrm{Ra}_x^{1/2} F(\xi, \eta), & \theta &= \frac{T = T_\infty}{T_w - T_\infty} \end{aligned}\right\} \tag{7}$$

where $\mathrm{Ra}_x = Kg\beta(T_w - T_\infty)x/\alpha v$ is the modified local Rayleigh number and ψ is the stream function, defined by

$$ru = \frac{\partial\psi}{\partial r} \quad \text{and} \quad rv = -\frac{\partial\psi}{\partial x} \tag{8}$$

which satisfies the continuity equation (Equation 1). Introducing the variable transformations (Equation 7) into Equation 8, we have

$$ru = \alpha\frac{\mathrm{Ra}_x}{x}\frac{\partial F}{\partial\eta} \tag{9}$$

and

$$rv = -\frac{\alpha r_0\,\mathrm{Ra}_x^{1/2}}{2rx}\left\{(1 - m)\left(\eta\frac{\partial F}{\partial n} - \xi\frac{\partial F}{\partial\xi}\right) - (1 + m)F\right\} \tag{10}$$

Notation

F	Transformed stream function defined in Equation 7
f_w	Blowing and suction parameter
Gr*	Modified local Grashof number, $\mathrm{Gr}^* = g\beta KK^*(T_w - T_\infty)/v^2$
g	Acceleration due to gravity
K	Permeability of the porous media
K^*	Inertial coefficient defined in Equation 4
m	Exponent introduced in Equation 6
q	Local heat transfer rate
r	Radial coordinate
r_0	Radial coordinate
Ra_x	Modified local Rayleigh number, $\mathrm{Ra}_x = Kg\beta(T_w - T_\infty)x/\alpha v$
T	Temperature
T_∞	Ambient constant temperature
T_w	Variable wall surface temperature
u, v	Reference velocity components in the x- and r-direction
V	Surface mass flux
x	Axial coordinate

Greek symbols

α	Equivalent thermal diffusivity of the fluid-saturated porous media
β	Expansion coefficient of fluid
δ	Fluid density
η	Pseudosimilarity variable defined in Equations 7
θ	Dimensionless temperature defined in Equations 7
λ	Exponent introduced in Equation 6
μ	Fluid viscosity
v	Fluid kinematic viscosity
ξ	Stretched streamwise coordinate defined by Equations 7
ψ	Stream function

Subscripts

∞	Quantity at infinity
w	Wall

The governing equations then turn into

$$F'' + 2\,\mathrm{Gr}^* F'F'' = \theta' \tag{11}$$

and

$$(1+\xi\eta)\theta'' + \left(\frac{1+m}{2} + \xi\right)F\theta' - mF'\theta = \frac{1-m}{2}\,\xi\left\{F'\frac{\partial\theta}{\partial\xi} - \theta'\frac{\partial F}{\partial\xi}\right\} \tag{12}$$

where $\mathrm{Gr}^*(=g\beta KK^*(T_w - T_\infty)/\nu^2)$ is the modified local Grashof number expressing the relative importance of the inertial effects, and the primes denote the differentiation of the respective functions with respect to η.

The corresponding boundary conditions become

$$\left.\begin{aligned} F(\xi,0) &= f_w, \quad \theta(\xi,0) = 1,\\ F'(\xi,\infty) &= 0, \quad \theta(\xi,\infty) = 0. \end{aligned}\right\} \tag{13}$$

where

$$f_w = -\frac{2a}{\alpha(1+m)}\left(\frac{g\beta KA}{\nu\alpha}\right)^{-1/2} \tag{14}$$

which is valid for $\lambda = (m-1)/2$. It is clear that f_w is positive for withdrawal and negative for blowing of fluid through the surface of the cylinder.

It can easily be seen that Equations 9 to 12 are local nonsimilarity equations. Possible similarity equations exist only for the case $\xi = 0$ for the flow along a vertical plate with vectored mass transfer. On the other hand, substitutions of $\mathrm{Gr}^* = 0$ and $f_w = 0$ reduce Equations 9 to 12 to the problem of Minkowycz and Cheng (1981) for the free-convection Darcy flow along a vertical cylinder, which they studied by an integral method. Later, the above problem for $m = 0$ was studied by Merkin (1986). In his analysis, Merkin investigated the problem by employing the perturbation technique for small and large values of the curvature parameter ξ. He also obtained the solution for a wide range of the curvature parameter ξ by the implicit finite-difference method. The present problem is composed of local similarity or nonsimilarity equations according to whether the right-hand sides of Equations 9 and 10 are neglected or retained for all values of m other than unity. According to Sparrow and Yu (1971), since local nonsimilarity solutions are more accurate than local similarity solutions, here we look for the local nonsimilarity solutions only. In the next section, we investigate the present problem by the use of the implicit finite-difference method together with the Keller box method of Keller (1978).

Once we know the velocity and temperature distributions from Equations 11 and 12 that satisfy the boundary conditions (Equation 13), we are in a position to know the local rate of heat transfer from

$$q(x) = -k_m\left(\frac{\partial T}{\partial r}\right)_{r=r_0} \tag{15}$$

which can be expressed in terms of the following dimensional variable:

$$q(x) = k_m A^{3/2}\left(\frac{\delta g\beta K}{\mu\alpha}\right)^{1/2} x^{(3m-1)/2}(-\theta(\xi,0)) \tag{16}$$

Results and discussion

Equations 9 to 12, together with the boundary conditions (Equation 13), have here been integrated by the implicit finite-difference scheme together with the Keller box method developed by Keller (1978). The numerical integrations start at $\xi = 0$, when F, F', θ, and θ' can be found from Equations 11 and 12, and then proceed in a step-size manner. The details of this method were very recently discussed by Hossain (1992); hence, for the sake of brevity they are not presented here. Total computations were carried out on a PC Epson 80286 computer, considering variable grids in the η-direction, defined by $\eta_j = \sinh j/a$. With $a = 25$, j is allowed to vary automatically so that η_∞ belongs to the interval $15 \le \eta_\infty \le 50$; this gives rise to convergent solutions with desired accuracy for given values of the parameters Gr^* and f_w. In order to assess the accuracy of the present method, we have compared our results for heat transfer at the surface for $\mathrm{Gr}^* = f_w = 0$ with those of Minkowycz and Cheng (1981) in Table 1 and have found them to be in excellent agreement. In Table 2, we again compare the present results for $\theta'(\xi,0)$ with those of Merkin (1986) and Minkowycz and Cheng (1981) for $\mathrm{Gr}^* = 0$, $f_w = 0$, and $m = 0$. It can be claimed that the present results are in good agreement with both Minkowycz and Cheng (1981) and Merkin (1986). It should be noted that Merkin (1986) used series expansions near the leading edge and far downstream, whereas Minkowcyz and Cheng (1981) employed the local nonsimilarity method. Table 2 also represents the values of $\theta'(\xi,0)$ for selected values of the modified Grashof number, Gr^*, ranging between 0 and 100, from which it can be observed that an increase in the value of

Table 1 Values of $-\theta'(\xi,0)$ for different values of m against ξ with $\mathrm{Gr}^* = 0$ and $f_w = 0$

ξ/m	0.0		0.25		0.5		1.0	
0.25	0.4899†	0.48996	0.6729†	0.67238	0.8167†	0.81593	1.046†	1.04528
0.50	0.5332†	0.53405	0.7175†	0.71660	0.8616†	0.86033	1.091†	1.09013
0.75	0.5747†	0.57677	0.7604†	0.75971	0.9052†	0.90381	1.135†	1.13383
1.00	0.6149†	0.61808	0.8023†	0.80162	0.9478†	0.94619	1.179†	1.17714
2.00	0.7668†	0.77420	0.9607†	0.96130	1.1100†	1.10866	1.345†	1.34317
3.00	0.9085†	0.91970	1.1100†	1.11069	1.2630†	1.26096	1.502†	1.49985
4.00	1.0440†	1.05877	1.2520†	1.25385	1.4090†	1.40702	1.654†	1.65008
5.00	1.1760†	1.19362	1.3910†	1.39251	1.5530†	1.54837	1.803†	1.79535
6.00	1.3050†	1.32548	1.5290†	1.52776	1.6960†	1.68607	1.952†	1.93669
7.00	1.4350†	1.45516	1.6670†	1.66038	1.8390†	1.82086	2.102†	2.07481
8.00	1.5650†	1.58320	1.8006†	1.79088	1.9840†	1.95327	2.253†	2.21024
9.00	1.6960†	1.70996	1.9470†	1.91965	2.1300†	2.08368	2.407†	2.34339
10.00	1.8300†	1.83570	2.0910†	2.04695	2.2800†	2.21240	2.564†	2.47457

† These values are from Minkowycz and Cheng (1981).

Table 2 Values of $-2^{1/2}\theta'(\xi, 0)$ for different values of Gr* against ξ with $m = 0$ and $f_w = 0$

ξ/Gr*		0.0		1.0	10.0	100.00
0.00	0.6276†	0.6276†	0.62755	0.51725	0.35446	0.21384
0.25	0.6928†	0.6933‡	0.69144	0.58406	0.42357	0.28621
0.50	0.7542†	0.7653‡	0.75261	0.64729	0.48820	0.35640
0.75	0.8127†	0.8170‡	0.81166	0.70791	0.55019	0.42562
1.00	0.8696†	0.8759†	0.86909	0.76666	0.61067	0.49394
2.00	1.0844†	1.0965‡	1.08636	0.98853	0.84351	0.75455
3.00	1.2848†	1.2996‡	1.29073	1.19816	1.06826	0.99769
4.00	1.4764†	1.4894‡	1.48759	1.40116	1.28621	1.22671
5.00	1.6631†	1.6683‡	1.67918	1.59917	1.49712	1.44481
6.00	1.8455†	1.8373‡	1.86646	1.79270	1.70126	1.65393
7.00	2.0294†	1.9988‡	2.04989	1.98196	1.89907	1.85540
8.00	2.2132†	2.1520‡	2.22972	2.16705	2.09103	2.05019
9.00	2.3985†	2.2980‡	2.40608	2.34805	2.27761	2.23903
10.00	2.5880†	2.4373‡	2.57905	2.52508	2.45919	2.42248

† These values are from Minkowycz and Cheng (1981).
‡ These values are from Merkin (1986).

Gr* leads to a decrease in the rate of heat transfer at the surface of the cylinder; and this trend of decrease reduces as the value of the parameter ξ goes higher. Finally, solutions are obtained for $m = 0$, 0.25, 0.5, and 1.0, for $f_w = 0, \pm 1$, and for ξ ranging between 0.0 and 15.0.

Figures 1 to 3 represent the value of the rate of heat transfer against ξ for selected values of Gr*, f_w, and m. From Figure 1 it may be observed that the rate of heat transfer decreases as Gr* increases at every selected value of m. On the other hand, an increase in the value of m leads to a rise in the value of the rate of heat transfer while Gr* remains fixed. Figures 2 and 3 show the effect of the vectored mass transfer on the rate of heat transfer at the surface of the cylinder for selected values of the parameters Gr* and m. From these figures, it may easily be concluded that withdrawal of fluid leads to increase and blowing of fluid leads to decrease in the rate of heat transfer at each selected value of Gr* and m.

Now we discuss the effects of the physical parameters Gr*, f_w, and m on the velocity and the temperature fields at $\xi = 1.0$. The representative velocity distribution for the non-Darcy flows along the surface of the vertical cylinder in absence as well as in the presence of the vectored mass transfer are shown graphically in Figures 4 and 5, respectively, for selected values of Gr* and m. The corresponding temperature distributions are shown in Figures 6 and 7. From Figure 5 it may be observed that the velocity profile decreases due to an increase either in Gr* or in m for the flow along the impermeable surface of the cylinder. It may also be observed from Figure 6 that withdrawal of fluid leads to increase and blowing leads to decrease of the velocity profiles in the flow field at each value of m. From

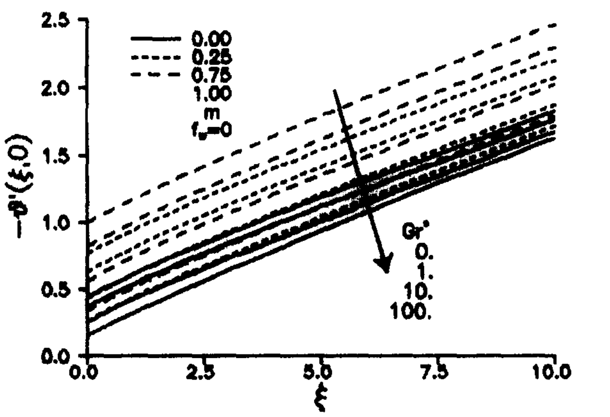

Figure 1 Local heat transfer against ξ for selected values of m and Gr*

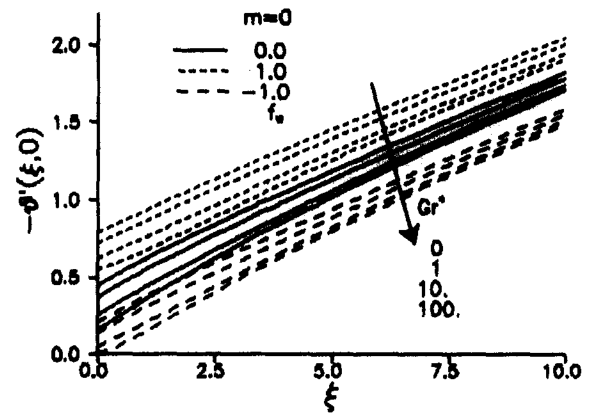

Figure 2 Local heat transfer against ξ for selected values of m and Gr*

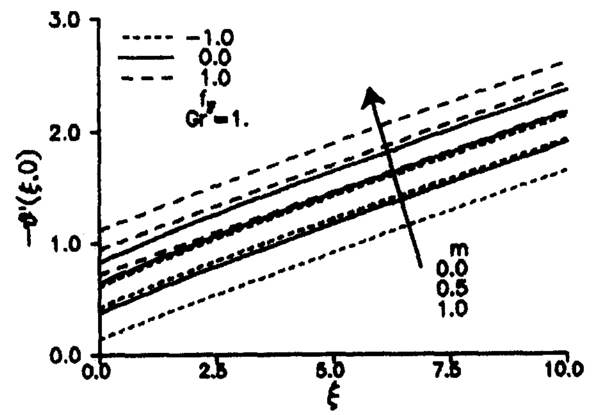

Figure 3 Local heat transfer against ξ for selected values of m and f_w and for Gr* = 1

Figure 7, it may be concluded that, in the absence of vectored mass transfer, increase of Gr* or m leads to decrease of the temperature distribution in the flow field. Finally, from Figure 7 we may conclude that, at every selected value of m, Gr*, and ξ, the temperature distribution increases when fluid is being withdrawn and decreases when fluid is being blown through the permeable surface of the cylinder.

From the present study, we have gained a better insight into the physics of the axisymmetric free convective flow in a porous medium. Whether or not the surface heat flux along a vertical circular cylinder increases, as compared with the case of Darcy free convection along a vertical flat plate with the same wall temperature variation, depends on the two opposing effects, namely, the transverse radial curvature effect to increase the heat flux and the non-Darcy porous inertia effect to decrease the heat flux. Furthermore, the influence of surface mass flux may also be quite significant. Thus, a realistic prediction of local heat transfer along a vertical circular cylinder can be made only when all these complex effects are taken into full consideration.

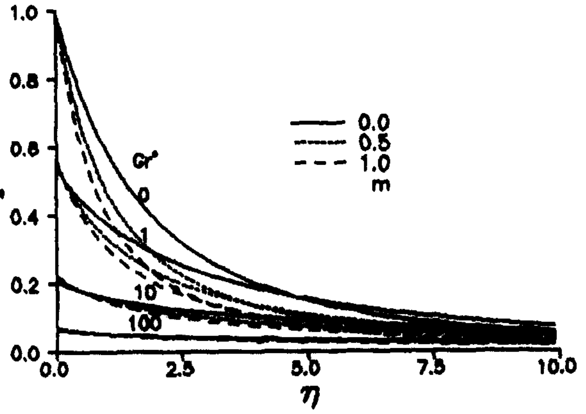

Figure 4 Velocity profiles against η for selected values of m and Gr* at $\xi = 1.0$ and $f_w = 0$

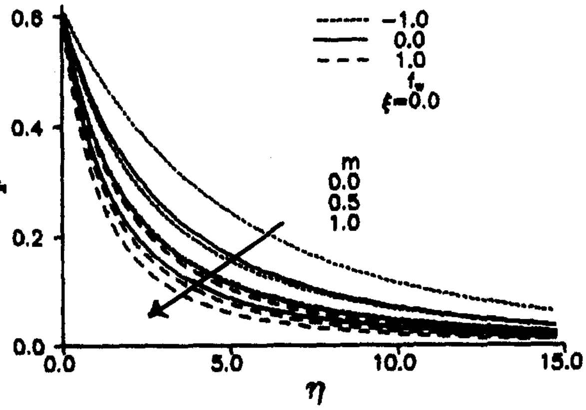

Figure 5 Velocity profiles against η for selected values of f_w and m for Gr* = 0 at $\xi = 1.0$

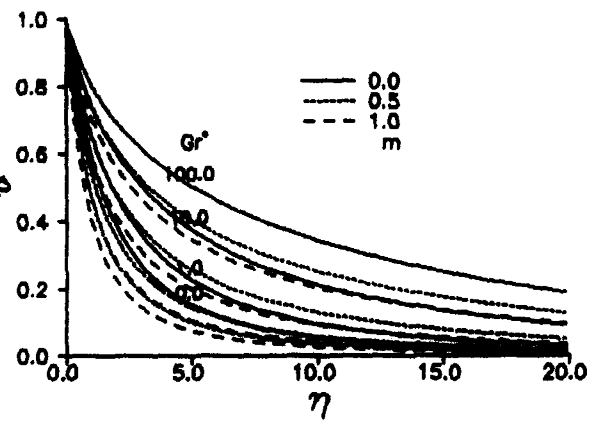

Figure 6 Temperature profiles against η for selected values of m and Gr* at $\xi = 1.0$ and $f_w = 0$

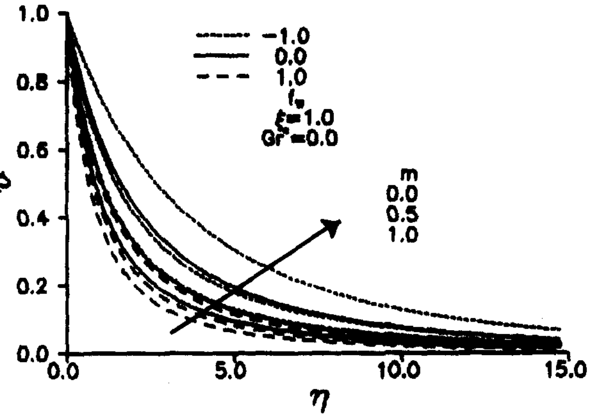

Figure 7 Temperature profiles against η for selected values of f_w and m for Gr* = 0 at $\xi = 1.0$

Conclusions

Extensive numerical integrations were carried out, using an implicit finite-difference technique together with the Keller box method, to investigate the problem of non-Darcy free convection along a vertical cylinder with surface mass flux. The numerical values are furnished for the wide ranges of the parameters associated with the porous inertia, transverse radial curvature, surface mass flux, and the wall temperature increase. Individual and combined effects of these parameters on the velocity and temperature fields are elucidated and presented graphically. From the present analysis we may conclude that (1) the rate of heat transfer decreases due to increase in Gr*, (2) withdrawal of fluid leads to an increase and the blowing of fluid leads to a decrease in the rate of heat transfer, (3) the velocity as well as the temperature profiles reduce due to increase in Gr*, and (4) withdrawal or blowing of fluid leads, respectively, to increase or decrease in the velocity as well as in the temperature fields.

References

Bejan, A. and Poulikakos, A. 1984. The non-Darcy regimes for vertical boundary layer natural convection in a porous media. *Int. J. Heat Mass Transfer*, **27**, 717–722

Cheng, P. 1977. The influence of lateral mass flux on free convection boundary layer in a saturated porous medium. *Int. J. Heat Mass Transfer*, **20**, 201–206

Cheng, P. 1978. Heat transfer in geothermal system. *Adv. Heat Transfer*, **14**, 1–105

Cheng, P. 1981. Thermal dispersion effects in non-Darcian convection flows in a saturated porous medium. *Lett. Heat Mass Transfer*, **8**, 267–270

Cheng, P. 1984. Natural convection in porous medium: External flows. NATO Advanced Study Institute, Izmir, Turkey

Hong, J. T., Yamada, Y., and Tien, C. L. 1987. Effect of non-Darcy and non-uniform porosity on vertical plate natural convection in porous medium. *J. Heat Transfer*, **109**, 356–362

Hong, J. T., Tien, C. L., and Kaviany, M. 1985. Non-Darcy effects on vertical plate natural convection in porous medium with high porosity. *Int. J. Heat Mass Transfer*, **28**, 2149–2157

Hossain, M. A. In press. Effect of transpiration on combined heat and mass transfer in mixed convection along a vertical plate. *Int. J. Energy Res.*, **16**

Hsu, T. C. and Cheng, P. 1985. Brinkman model for free convection about a flat plate in a porous medium. *Int. J. Heat Mass Transfer*, **28**, 683–697

Ingham, D. B. 1986. The non-Darcy free convection boundary layer on axisymmetric and two-dimensional bodies of arbitrary shape. *Int. J. Heat Mass Transfer*, **29**, 1759–1763

Keller, H. B. 1978. Numerical methods in boundary layer theory. *Annu. Rev. Fluid Mech.*, **10**, 417–433

Kumari, M., Pop, I., and Nath, G. 1990. Non-similar boundary layer for non-Darcy mixed convection flow about a horizontal surface in a saturated porous medium. *Int. J. Eng. Sci.*, **28**, 253–263

Lai, F. C. and Kulacki, F. A. 1990. The influence of surface mass flux on mixed convection over horizontal plates in saturated porous media. *Int. J. Heat Mass Transfer*, **33**, 576–579

Merkin, J. H. 1986. Free convection from vertical cylinder embedded in a saturated porous medium. *Acta Mechanica*, **62**, 19–28

Minkowycz, W. J. and Sparrow, E. M. 1974. Local nonsimilarity solutions for natural convection on a vertical cylinder. *J. Heat Transfer*, **96**, 178–183

Minkowycz, W. J. and Cheng, P. 1981. Free convection about a vertical cylinder embedded in a porous medium. *Int. J. Heat Mass Transfer*, **19**, 805–812

Minkowycz, W. J., Cheng, P., and Mialem, F. 1985. The effect of surface mass transfer on buoyancy induced Darcian flow adjacent to a horizontal heated surface. *Int. Comm. Heat Mass Transfer*, **12**, 55–65

Plumb, O. A. and Huenefeld, J. C. 1981. Non-Darcy natural convection from heated surfaces in saturated porous medium. *Int. J. Heat Mass Transfer*, **24**, 765–768

Sparrow, E. M. and Yu, H. S. 1971. Local nonsimilarity thermal boundary layer solutions. *J. Heat Transfer*, **93**, 328–334

Vasantha, R., Pop, I., and Nath, G. 1986. Non-Darcy natural convection over a slender vertical frustram of a cone in a saturated porous medium. *Int. J. Heat Mass Transfer*, **29**, 153–156